J Neurophysiol 102: 2800–2815, 2009.
First published September 9, 2009; doi:10.1152/jn.00284.2009.

On the Open-Loop and Feedback Processes That Underlie the Formation of Trajectories During Visual and Nonvisual Locomotion in Humans

Quang-Cuong Pham[1] and Halim Hicheur[1,2]

[1]*Laboratoire de Physiologie de la Perception et de l'Action, Collège de France-Centre National de la Recherche Scientifique, Unité Mixte de Recherche 7152, Paris, France; and* [2]*Hertie Institute for Clinical Brain Research, Department of Cognitive Neurology, University Clinic Tuebingen, Germany*

Submitted 31 March 2009; accepted in final form 3 September 2009

Pham QC, Hicheur H. On the open-loop and feedback processes that underlie the formation of trajectories during visual and nonvisual locomotion in humans. *J Neurophysiol* 102: 2800–2815, 2009. First published September 9, 2009; doi:10.1152/jn.00284.2009. We investigated the nature of the control mechanisms at work during goal-oriented locomotion. In particular, we tested the effects of vision, locomotor speed, and the presence of via points on the geometric and kinematic properties of locomotor trajectories. We first observed that the average trajectories recorded in visual and nonvisual locomotion were highly comparable, suggesting the existence of vision-independent processes underlying the formation of locomotor trajectories. Then by analyzing and comparing the variability around the average trajectories across different experimental conditions, we were able to demonstrate the existence of on-line feedback control in both visual and nonvisual locomotion and to clarify the relations between visual and nonvisual control strategies. Based on these insights, we designed a model in which maximum-smoothness and optimal feedback control principles account, respectively, for the open-loop and feedback processes. Taken together, the experimental and modeling findings provide a novel understanding of the nature of the motor, sensory, and "navigational" processes underlying goal-oriented locomotion.

INTRODUCTION

The study of human locomotion includes different levels of analysis from the neuronal discharges governing the muscular activity (see Capaday 2002 for a review) to the mechanical forces exerted on the ground, allowing the propulsion of the body. While the understanding the locomotor behavior per se greatly benefited from such analyses, only few studies were devoted to clarify the relations between the mechanical, sensorimotor aspects of locomotion and its "navigational," cognitive components (see Hicheur et al. 2005a for a review). Yet it is critical to provide an integrative view of locomotion, associating our knowledge of the mechanical, sensorimotor, and navigational components of locomotion within a unifying framework: indeed, these different components are necessarily taken into account by the central nervous system (CNS) for the production of the locomotor commands.

It is well known in the field of motor control that the same shape can be implemented by various effectors (the "principle of motor equivalence") (see Bernstein 1967). For example, one can draw the letter A with the finger, the hand, or even by running on a flat surface. Following this idea, we have previously tested the hypothesis that the control of locomotor trajectories obey the same laws as those originally formulated for hand movements, such as the 2/3 power law relating the path curvature to the tangential velocity of the body (Hicheur et al. 2005b; see also Olivier and Crétual 2007; Vieilledent et al. 2001). While this hypothesis could be partially supported, more general principles accounting for the formation of whole-body trajectories remained to be investigated in particular those based on the optimal nature of motor control.

We have thus recently undertaken the study of *goal-oriented* locomotion in a task involving walking toward and through a distant doorway (Arechavaleta et al. 2006; Hicheur et al. 2007). While neither the paths nor the walking speeds were constrained, we observed that humans generated *stereotyped* trajectories at both the geometric (the paths) and kinematic (the velocity and turning profiles) levels, which contrasted with a large variability of feet placements (Hicheur et al. 2007). This indicated that locomotion is not controlled as a mere *sequence of steps*: rather higher-level cognitive strategies govern the formation of *whole-body trajectories*. While providing an integrative view on human locomotion by addressing both its step- and trajectory-related aspects, this approach also brought about a new understanding of locomotion that takes advantage of the recent theoretical advances in *computational motor control* (for reviews, see Jordan and Wolpert 1999; Todorov 2004). A further step in this direction was made when, based on the observation that locomotor trajectories were particularly smooth, we reported that a maximum-smoothness model, originally formulated for hand movements (Flash and Hogan 1985), could also predict locomotor trajectories with great accuracy (Pham et al. 2007).

Our ambition in the present article is to further develop this integrative and computational approach to provide a deeper understanding of the *control mechanisms* at work during the production of locomotor trajectories in a goal-oriented task. For instance, the maximum smoothness model, which is deterministic, could not explain the *variability* around the average trajectories. Yet the analysis of movement variability is crucial for the understanding of human movements. In the particular case of locomotion, Winter and Eng (1995) showed, by studying the variability of the knee and hip angles, that the "controlled variable" is rather the *sum* of these two angles than any of them taken separately (in other words, a synergetic control of the joint angles). More recently, the optimal feedback control theory, which specifically relies on the analysis of movement variability, was proposed as a general theory of human movements (Todorov and Jordan 2002).

Address for reprint requests and other correspondence: Q.-C. Pham, Laboratoire de Physiologie de la Perception et de l'Action, Collège de France Centre National de la Recherche Scientifique Unité Mixte de Recherche 7152, 11 Place Marcelin Berthelot, 75005 Paris, France (E-mail: cuong.pham@normalesup.org).

In the present article, we therefore not only study the average locomotor trajectories but also the *variability profiles* (how variability evolves in time). To discover the fine structure of these variability profiles, we adopted a *differential approach*, where variability profiles in different experimental conditions were compared. In particular, we varied the visual condition (walking with eyes open or closed), the speed condition (walking at normal or fast speed), and the presence of via points along the locomotor path. Yet the comparison of the variability in two different conditions can only be fruitful if this variability is structured around the same average behavior. We thus conducted a first experiment where we tested, for a large range of spatial targets, whether the average trajectories in visual and nonvisual locomotion were similar or not. In the subsequent experiments, we used a more restricted number of spatial targets but a larger number of repetitions per target to examine and compare with better confidence the variability profiles.

A basic assumption of our study is that, theoretically, the control mechanism governing the formation of locomotor trajectories may be divided in two parts (Fig. 1): an *open-loop process*, which can be executed independently of sensory feedbacks, and a *feedback module*, which can modify the open-loop process based on sensory feedbacks to correct the random perturbations that may occur during task execution. Based on the experimental results, we argue that on-line feedback control is present in *both* visual and nonvisual locomotion and suggest the relations between the visual and nonvisual control strategies. We then investigate the precise nature of the on-line feedback control and discuss two competing hypotheses: the "desired trajectory" hypothesis, which assumes two separate stages in the production of a movement: a planning stage when a desired optimal trajectory is computed and an execution stage when this desired trajectory is implemented with "trajectory tracking" mechanisms correcting any deviation away from the desired trajectory; and the optimal feedback control hypothesis (Todorov and Jordan 2002), which states that "deviations from the average trajectory are corrected only when they interfere with task performance" (*goal-directed* corrections, as opposed to desired-trajectory-related corrections).

To test these hypotheses in a direct way, we also consider several *models* of trajectory formation relying on either purely open-loop or optimal feedback control. By analyzing and comparing the models' predictions with experimental data (in terms of both average trajectories and variability profiles), we provide evidence that locomotor trajectories, even in the absence of vision, are controlled in an optimal way.

EXPERIMENTAL METHODS

Four experiments were conducted involving a total of 22 healthy subjects. Subjects gave their informed consent prior to their inclusion in the study. The experiments conformed to the Code of Ethics of the Declaration of Helsinki. In *experiment 1,* we studied the effect of vision on the average trajectories and on the *magnitude* of the variability around the average trajectory. *Experiment 2* was designed to more specifically examine the *time course* of the variability (variability profile) in the visual (VI) and nonvisual (NV) conditions. *Experiment 3* addressed the influence of speed and *experiment 4* aimed at assessing the desired trajectory hypothesis in the context of locomotion.

Materials

A number of light-reflective markers were attached to the subject: 42 in *experiments 1–3* (allowing full-body movement capture), and 2 in *experiment 4* (the 2 shoulder markers). The three-dimensional (3D) positions of these markers were recorded at a 120-Hz sampling frequency using an optoelectronic Vicon V8 motion-capture system wired to 12 cameras. To study whole-body trajectories in space, we used the midpoint between the left and right shoulder markers that were located on the left and right acromions, respectively (see Hicheur et al. 2007). In *experiment 2,* we used in addition the left and right heel markers to compute the number of steps.

In all trials, the target was indicated by a cardboard arrow of dimension 1.20 × 0.25 m (length and width, respectively). The arrow was placed at a specific (x,y) position in the motion capture space with an orientation α (Fig. 2, *A–C*).

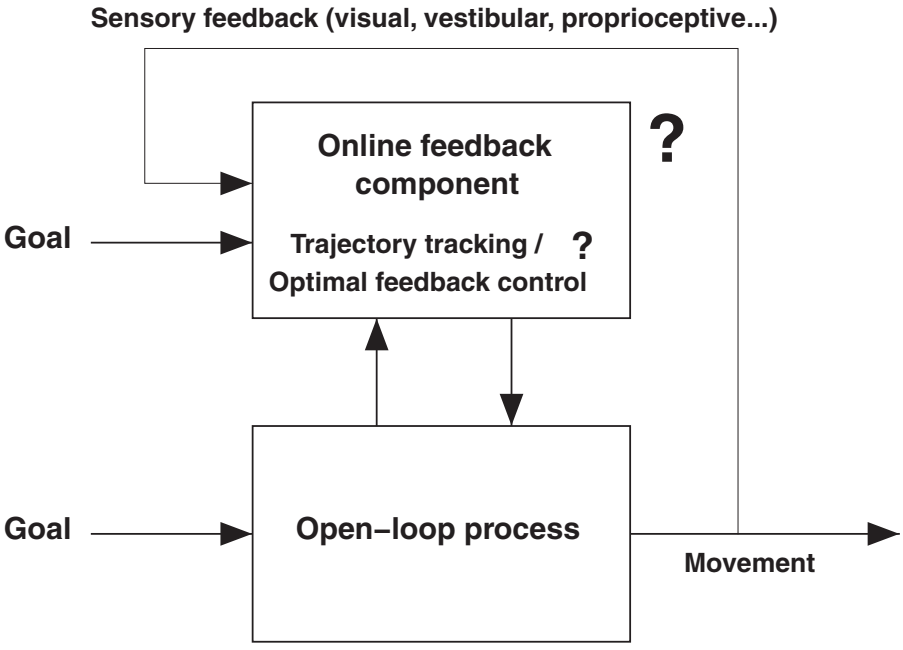

FIG. 1. Sketch of a general controller, including an open-loop process and a feedback module. The question marks indicate some of the issues investigated in the present article: namely, does on-line feedback control exist in visual and nonvisual locomotion and what is the precise nature of the feedback control scheme, trajectory tracking or optimal feedback control?

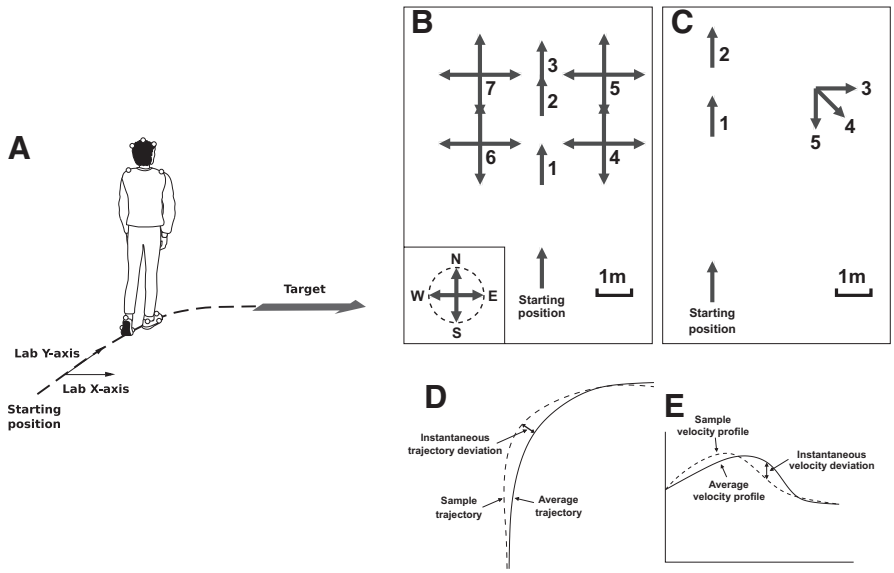

FIG. 2. *A*: experimental protocol: the subject had to start from a fixed position in the laboratory and walk toward a distant arrow placed on the ground. He had to enter the arrow by the shaft and stop above the arrow head. *B*: spatial layout of the 19 targets in *experiment 1*: each target was referred to by a number (1–7) indicating its position and by a letter (N: north, S: south, E: east, W: west) indicating its orientation. *C*: spatial layout of the 5 targets in *experiment 2*. *D*: the instantaneous trajectory deviation [TD(t)] measures the variability of actual trajectories around the average trajectory (*Eq. 1*). *E*: the instantaneous velocity deviation [VD(t)] measures the variability of actual velocity profiles around the average velocity profile (*Eq. 5*).

Experiments 1–3 took place in a laboratory of dimensions ~10 × 10 × 5 m (length, width, and height, respectively). *Experiment 4* was carried out in a smaller laboratory (~6 × 8 × 4 m).

Experiment 1

Fourteen male subjects participated in this experiment. The mean age, height, and weight of the subjects were, respectively, 24.6 ± 3.2 yr, 1.80 ± 0.04 (SD) m, and 73.3 ± 5.7 kg.

In each trial, the subject had to start from a fixed position in the laboratory and to walk toward a distant target indicated by an arrow (Fig. 2*A*). We constrained the subject's initial walking direction by asking him to start at position (0,−1 m) and to walk the first meter [from (0,−1 m) to (0,0)] orthogonally to the x axis (Fig. 2, *A–C*). After crossing the x axis, no specific restriction relative to the path to follow was provided to the subject. We imposed the subject's final walking direction by asking the subject to enter the arrow by the shaft and to stop walking above the arrowhead.

The subject walked either with eyes open (VI) or closed (NV). In this experiment, he was asked to walk at his preferred normal speed. In condition VI, the arrow was visible throughout the whole movement. In condition NV, the subject first observed the arrow while standing at the starting position. This observation period typically lasted <3 s. When the subject was ready, he closed his eyes and attempted to complete the task without vision. The subject was asked to complete the task with the same initial and final constraints as in condition VI—namely, walk the first meter orthogonally to the x axis, enter the arrow by the shaft, and stop above the arrowhead. Right after the observation period, the experimenter removed the arrow to avoid tactile feedbacks. Once the subject had completely stopped, he was asked to keep his eyes closed while the experimenter took his hand and guided him randomly for a few seconds in the laboratory before stopping at a random position. The subject was then allowed to re-open his eyes and to go back to the starting position. This procedure prevented the subject from acquiring visual feedbacks during both task and posttask periods (avoiding in this way spatial calibrations of the room using kinesthetic cues). The trials were randomized to avoid learning effects for a particular condition or target. The subject completed two to three trials before the experiment actually started to be familiar with the task and to dispel any fear of hitting the walls during the nonvisual trials (the distance between the most distant target and the wall was ~3 m).

The angular displacement of the body in space induced by the different orientations of the arrow ranged between −180 and 180° (Fig. 2*B*). Three targets were placed straight ahead of the subject (straight targets), while the others were placed on the side (angled targets).

The three straight targets were used for all subjects. A subgroup of six subjects walked toward the angled targets located on the left, while the remaining eight subjects walked toward the angled targets on the right. Thus each subject generated 66 trajectories corresponding to 11 spatial targets (3 straight + 8 angled) × two conditions (VI and NV) × 3 trials so that a total of 924 trajectories (14 subjects × 66 trials) were recorded for this experiment.

Experiment 2

The methodology used in this experiment was the same as in *experiment 1* except that here we examined specifically the time course of the variability profiles in conditions VI and NV. We increased the number of repetitions to eight per condition and target. This allowed us to study *intrasubject* variability profiles with a greater reliability.

This experiment was realized in the same laboratory as *experiment 1*. We tested five male subjects, four of whom had already participated in *experiment 1,* which took place 12 mo before. The mean age, height, and weight of the subjects were, respectively, 29.2 ± 4.2 yr, 1.80 ± 0.06 m, and 68.8 ± 5.1 kg.

We reduced the number of targets to five: two straight targets and three angled targets (Fig. 2*C*). Thus each subject executed 80 trials (2 visual conditions × 5 targets × 8 repetitions). As in *experiment 1,* the trials were randomized to reduce learning effects. A total of 400 trajectories (5 subjects × 80 trials) were recorded.

Experiment 3

The methodology and the protocol used in this experiment were the same as in *experiment 2* except that we varied the speed instruction: subjects were asked to walk either at their preferred speed (normal speed, NS) or at a higher speed (fast speed, FS). Vision was available in both speed conditions.

We tested five male subjects in this experiment, three of whom had already participated in *experiment 1,* which took place 12 mo before. The mean age, height, and weight of the subjects were, respectively, equal to 25.8 ± 3.6 yr, 1.80 ± 0.02 m, and 75.9 ± 3.7 kg. As in *experiment 2,* a total of 400 trajectories (5 subjects × 2 speed conditions × 5 targets × 8 repetitions) were recorded.

Experiment 4

This simple experiment adapted a hand movement experiment from (Todorov and Jordan 2002) to the context of locomotion to test the "desired trajectory" hypothesis (see INTRODUCTION).

The experiment was divided in three sessions separated by several hours. In the first session, the task was the same as in the previous experiments, namely, walking toward a distant arrow. We used only one target, similar to target 5 in Fig. 2*C*. The subject performed 10 trials in this session all with vision and at normal speed. We then computed the average trajectory $[x_{av}(t),y_{av}(t)]$, $0 \leq t \leq 1$ across these 10 trials. We denoted, respectively, by P_1, P_2, and P_3 the spatial positions $[x_{av}(0.33),y_{av}(0.33)]$, $[x_{av}(0.5),y_{av}(0.5)]$, and $[x_{av}(0.67),y_{av}(0.67)]$.

In the second session, we placed a piece of black tape on the ground at position P_2. The subject was then asked, as in the first session, to walk toward the distant arrow. In addition, he had now to go through the via point indicated by the piece of black tape. Again the subject had to perform 10 repetitions. The third session was similar in all aspects to the second session except that the subject had to go successively through the *three* via points, P_1–P_3.

We tested five subjects, three males and two females. None had participated in the previous experiments. The mean age, height, and weight of the subjects were, respectively, equal to 30.2 ± 3.8 yr, 1.74 ± 0.08 m, and 68.0 ± 11.9 kg. A total of 150 trajectories (5 subjects × 3 sessions × 10 repetitions) were recorded.

Data analysis

All the data analyses below were performed with the free software GNU Octave unless otherwise stated.

Computation of the trajectories

The beginning ($t = 0$) of each trajectory was set to the time instant when the subject crossed the x axis. To have the same criterion for the VI and NV conditions, the end of each trajectory ($t = 1$) was set to the time instant when the subject's speed became <0.06 m/s (this value was <5% of the average nominal walking speed). We chose this strictly positive threshold because even when the subject had completely stopped, the speed of their shoulders' midpoint was not exactly zero due to the small residual movements of the upper body.

When a derivative of the position (velocity, acceleration, etc.) was needed, a second-order Butterworth filter with cut-off frequency 6.25 Hz was applied before the derivation.

Average trajectories, variability profiles, velocity profiles

For a given target, the average trajectory $[x_{av}(t), y_{av}(t)]$ was defined by

$$x_{av}(t) = \frac{1}{N}\sum_{i=1}^{N} x_i(t);\ y_{av} = \frac{1}{N}\sum_{i=1}^{N} y_i(t) \qquad (1)$$

where N corresponds to the number of trajectories recorded for this target ($n = 42$ for the intersubject analysis of *experiment 1; n* = 8, 8, and 10, respectively, for the intrasubject analyses of *experiments 2–4*).

To measure the variability of actual trajectories around the average trajectory, we defined the instantaneous trajectory deviation (TD) at time t as (see Fig. 2*E* for illustration)

$$\mathrm{TD}(t) = \sqrt{\frac{1}{N-1}\sum_{i=1}^{N}[x_i(t) - x_{av}(t)]^2 + [y_i(t) - y_{av}(t)]^2} \qquad (2)$$

We then defined the maximum trajectory deviation (MTD) by

$$\mathrm{MTD}(t) = \max_{0\leq t\leq 1} \mathrm{TD}(t) \qquad (3)$$

Variance ellipses were calculated by principal component analysis: the variance ellipse at time t is centered at $[x_{av}(t), y_{av}(t)]$ and its orientation and size indicate how the $[x_i(t), y_i(t)]$ ($i = 1, \ldots, N$) are distributed around $[x_{av}(t), y_{av}(t)]$. Note that $r_1(t)^2 + r_2(t)^2 = \mathrm{TD}(t)^2$ where r_1 and r_2 are the lengths of the ellipse's semi major and semi minor axes (Pham et al. 2007).

The variability profiles and the variance ellipses of *experiment* 4 were computed differently, in a manner similar to that described in the legend of Fig. 5 in Liu and Todorov (2007). This was done to better assess the effects of the *spatial* via points.

If a set of trajectories have similar geometric paths, it makes sense to study also the variability of their velocity profiles. For this, we defined the normalized velocity profile v_i and the average normalized velocity profile v_{av} as follows

$$v_i = \frac{\sqrt{\dot{x}_i^2 + \dot{y}_i^2}}{\int_0^1 \sqrt{\dot{x}_i^2 + \dot{y}_i^2}\,dt};\ v_{av} = \frac{1}{N}\sum_{i=1}^{N} v_i \qquad (4)$$

Next, the instantaneous velocity deviation (VD) can be defined by

$$\mathrm{VD}(t) = \sqrt{\frac{1}{N-1}\sum_{i=1}^{N}[v_i(t) - v_{av}(t)]^2} \qquad (5)$$

Note that because the velocity profiles were normalized, v_i and VD have no units.

Comparison of trajectories in two conditions

For comparing the average trajectories recorded in two different conditions, say A and B, we defined, for each target, the instantaneous trajectory separation (TS) by

$$\mathrm{TS}_{A/B}(t) = \sqrt{[x_A(t) - x_B(t)]^2 + [y_A(t) - y_B(t)]^2} \qquad (6)$$

where (x_A,y_A) and (x_B,y_B) denote the average trajectories respectively in condition A and in condition B.

We then defined the maximum trajectory separation (MTS) by

$$\mathrm{MTS}_{A/B}(t) = \max_{0\leq t\leq 1} \mathrm{TS}_{A/B}(t) \qquad (7)$$

Targets pooling in experiment 1

In *experiment 1,* six subjects walked toward targets located on their left and eight subjects walked toward targets located on their right (see Fig. 2*B*). We found no significant effect of the side on the parameters of interest: for instance, the $\mathrm{MTS}_{L/R}$ (MTS between the average trajectory of the left trajectories and that of the right trajectories) was smaller than the MTD_R (MTD of the right trajectories) in both conditions VI and NV. In the two-way ANOVA test with replications where the factors were the measure ($\mathrm{MTS}_{L/R}$ vs. MTD_R) and the visual condition, the effect of the measure was significant [$F(1,40) = 37.4$, $P < 0.05$], and there was no significant interaction effect [$F(1,40) = 2.82$, $P > 0.05$]. Thus for all the following analyses, we flipped the left trajectories toward the right and pooled them together with their symmetrical trajectories (trajectories of target 4 with those of target 6, trajectories of target 5 with those of targets 7).

Step-level analysis in experiment 2

In Hicheur et al. (2007), we carried out an extensive step-level analysis to compare the variability of feet placements with that of whole-body trajectories. Here the purpose of the step-level analysis was solely to assess whether the subjects used a *steps-counting*

strategy in the nonvisual trials, which may consist of count the number steps executed in one visual trial and reproduce the same number of steps in the corresponding nonvisual trials.

For this, we considered the z coordinates of the left and right heel markers as functions of time. The total number of local maxima of these two signals then gave the number of steps (SN, steps number) executed by the subject. The trial-to-trial variability of this quantity was given by the steps number deviation (SND)

$$\mathrm{SND} = \sqrt{\frac{1}{N-2}\sum_{i=2}^{N}(\mathrm{SN}_i - \mathrm{SN}_{\mathrm{av}})^2} \quad (8)$$

where N is the number of repetitions ($n = 8$ here). Note that we discarded the first trial in the computation of both the average and the SD of the SNs. The discard was done to include only the nonvisual trials that were preceded by at least one visual trial (this is required by the steps-counting strategy, see preceding text). For symmetry, we discarded also the first visual trial.

Linearity coefficient

To measure how close a variability profile is from a linear profile, we defined a linearity coefficient (LC). The LC of a time series $[y_i(t_i), 1 \leq i \leq N]$ quantifies the distance between this time series and its best linear approximation $y = ct$, with $0 \leq \mathrm{LC} \leq 1$ and $\mathrm{LC} = 1$ for a linear profile. First, the optimal coefficient c was computed by

$$c = \left(\sum_{i=1}^{T} y_i t_i\right) \Big/ \left(\left(\sum_{i=1}^{T} t_i^2\right)\right) \quad (9)$$

Next, the squared approximation error was given by

$$\mathrm{ESS} = \sum_{i=1}^{T}(y_i - ct_i)^2 \quad (10)$$

Finally, the LC was given by

$$\mathrm{LC} = 1 - \mathrm{ESS}/\mathrm{Var}(y) \quad (11)$$

Statistical tests

Student's t-test and ANOVA tests were performed with Gnumeric (GNOME Foundation, Cambridge, MA) while Tukey tests were performed with Matlab (The MathWorks, Natick, MA). The level of significance of the tests was set to $P < 0.05$.

In *experiment 1,* paired t-test were performed to compare the MTDs in conditions VI and NV or the MTD in condition VI with the $\mathrm{MTS}_{\mathrm{VI/NV}}$. In both cases, the values to be compared were paired with respect to the target (df = 10).

In *experiment 2,* we used two-way ANOVA tests with replications (or 2-way repeated-measures ANOVA) to assess the effect of the visual condition on the MTDs and on the SNDs. The first factor of the test was the visual condition (df = 1), and the second factor was the target (df = 4).

Two-way ANOVA tests with replications were used to assess the effect of the speed instruction on the actually measured average speeds or the MTDs. The first factor of the test was the speed condition (df = 1), and the second factor was the target (df = 4). We also compared the MTD in condition NS with the $\mathrm{MTS}_{\mathrm{NS/FS}}$ using a similar two-way ANOVA test.

In *experiment 4,* we used a one-way ANOVA test with replications to assess the effect of the via-point condition (no, 1, or 3 via points) on the MTDs. If a significant effect was found, we performed post hoc Tukey tests to assess the effect of the via-points within each pair of conditions.

EXPERIMENTAL STUDY

Results

VISION DOES NOT AFFECT THE AVERAGE TRAJECTORIES (*EXPERIMENT 1*). Average trajectories in the VI and NV conditions were similar both at the geometric level (the paths) and the kinematic level (the velocity profiles): see Fig. 3, *A, 1* and *2, B, 1* and *2,* and *C, 1* and *2*. Specifically, the NV trajectories displayed all the typical features observed in the VI trajectories: straight paths for straight targets, smoothly curved paths for angled targets, inverse relationship between velocity and curvature. The similarity was particularly striking even for the most angled targets such as 4W, 5W, 4S, and 5S.

More quantitatively, the average $\mathrm{MTS}_{\mathrm{VI/NV}}$ across targets was 0.30 ± 0.10 m (or $5.7 \pm 2.9\%$ of trajectory length). There was no statistically significant difference between the $\mathrm{MTS}_{\mathrm{VI/NV}}$ and the $\mathrm{MTD}_{\mathrm{VI}}$, which was 0.31 ± 0.10 m (paired 2-tailed t-test, df = 10, $t = -0.18$, $P > 0.05$). In other words, the difference between the average trajectories in the two conditions was of the same magnitude as the variability within condition VI.

VISION AFFECTS THE VARIABILITY AROUND THE AVERAGE TRAJECTORIES (*EXPERIMENTS 1* AND *2*). *Intersubject variability (experiment 1).* While the average trajectories in the VI and NV conditions were similar, the absence of visual feedbacks yielded large differences in terms of the variability profiles. In *experiment 1,* the average $\mathrm{MTD}_{\mathrm{NV}}$ across targets was equal to 0.74 ± 0.13 m, which was significantly larger than the $\mathrm{MTD}_{\mathrm{VI}}$ (paired 1-tailed t-test, df = 10, $t = 16.0$, $P < 0.05$). Moreover, the shapes of the intersubject variability profiles differed greatly between the two conditions (this is further discussed later).

*Intrasubject variability (*experiment 2*).* The preceding observation that the intersubject variability was larger in nonvisual locomotion than in visual locomotion was confirmed in *experiment 2* on an intrasubject basis (Fig. 4*C*). In the two-way ANOVA test where the factors were the visual condition and the target, the main effect of the visual condition on the MTD was found to be significant [$F(1,40) = 86.1$, $P < 0.05$], and there was no significant interaction effect [$F(4,40) = 0.61$, $P > 0.05$].

We noted, however, that the difference between the average trajectories of conditions VI and NV in *experiment 2* was larger than the corresponding values reported in *experiment 1*: here the average $\mathrm{MTS}_{\mathrm{VI/NV}}$ across targets and subjects was 0.54 ± 0.25 m (Fig. 4*C*), whereas the average $\mathrm{MTS}_{\mathrm{VI/NV}}$ across targets was 0.30 ± 0.10 m in *experiment 1*. This difference could be explained by the fact that in *experiment 2,* the average trajectories were computed across 8 trials (intrasubject average), whereas in *experiment 1,* these were computed across 42 trials (intersubject average). Had we grouped together the five subjects of *experiment 2* (thus averaging across 40 trials), this would yield a value of 0.35 ± 0.12 m for $\mathrm{MTS}_{\mathrm{VI/NV}}$, a value comparable to that of *experiment 1* given in the preceding text.

NO STEPS-COUNTING STRATEGY IN NONVISUAL TRIALS (*EXPERIMENT 2*). It could be argued that despite the randomized order of the trials, the subjects may have used a steps-counting strategy (see METHODS). Such a strategy would imply a low trial-to-trial variability in the number of steps in condition NV. We observed, on the contrary, that the average SND across targets and subjects was 0.79 in condition NV, which was higher than in condition VI (SND = 0.54), where arguably no

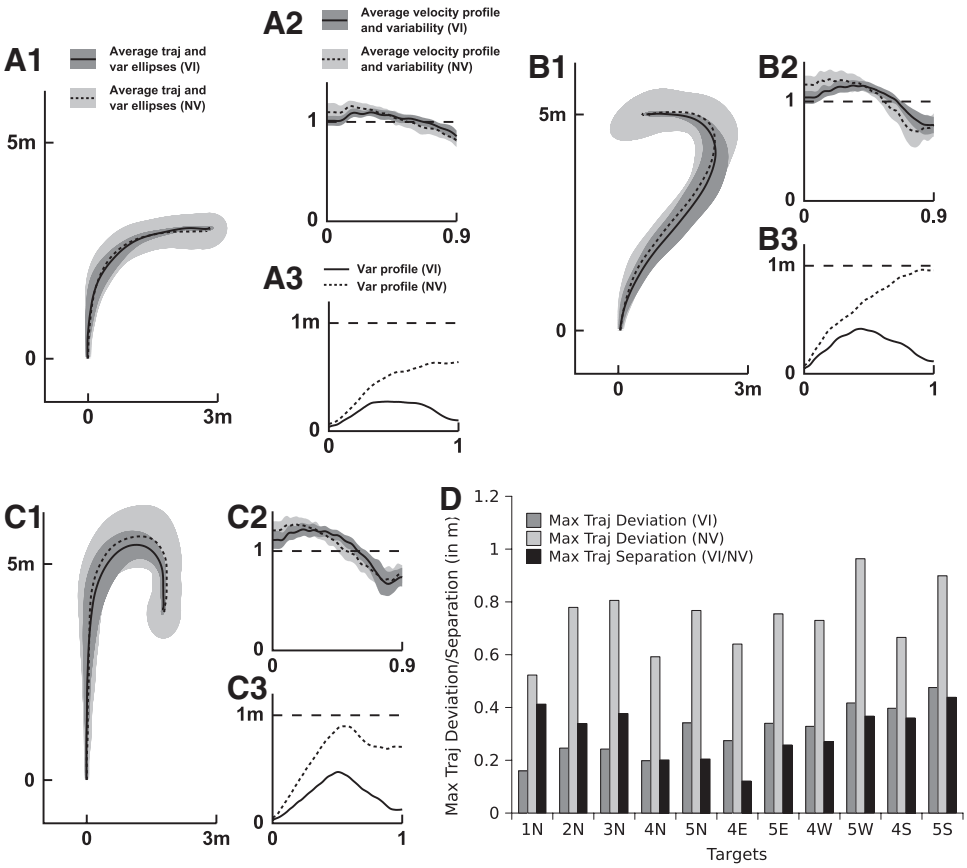

FIG. 3. *Experiment 1*: comparison of locomotor trajectories in the visual (VI: plain lines) and nonvisual (NV: dashed lines) conditions. *A*: comparison for target 4E. *A1*: geometric paths of the average trajectories. Variance ellipses around the average trajectory at every time instant (see METHODS) are shaded in dark gray (VI) and light gray (NV). *A2*: average velocity profiles. The velocity profiles were normalized so that their average values over the movement duration equals 1 (see METHODS). SDs around the average velocity profiles are shaded in dark gray (VI) and light gray (NV). *A3*: variability profiles [TD(t)]. *B*: same as in *A* but for target 5W. *C*: same as in *A* but for target 5S. *D*: maximal trajectory deviation/separation (MTD/MTS) in meters: MTD in condition VI (dark gray bars), MTD in condition NV (light gray bars), MTS between the average trajectory of VI and NV (black bars).

steps-counting strategy was used. In the two-way ANOVA test where the factors were the visual condition and the target, the main effect of the visual condition on the SND was found to be significant [$F(1,40) = 7.6$, $P < 0.05$], and there was no significant interaction effect [$F(4,40) = 0.82$, $P > 0.05$].

BUMP-SHAPE OF THE VARIABILITY PROFILES IN VISUAL LOCOMOTION (*EXPERIMENT 2*). We noted that in both conditions VI and NV, the variability was low at the beginning of the movement. This is related to the fact that for given a target, the subject started all the trials from the same starting position.

In condition VI, the variability was also close to zero at the end of the movement. This is because when vision was available, the subject could complete all the trials successfully by stopping at the requested final position. Regarding the middle part of the variability profiles, one may distinguish between the straight targets and the angled targets. For the former, the variability was close to zero during the whole movement (see the plain lines in Fig.

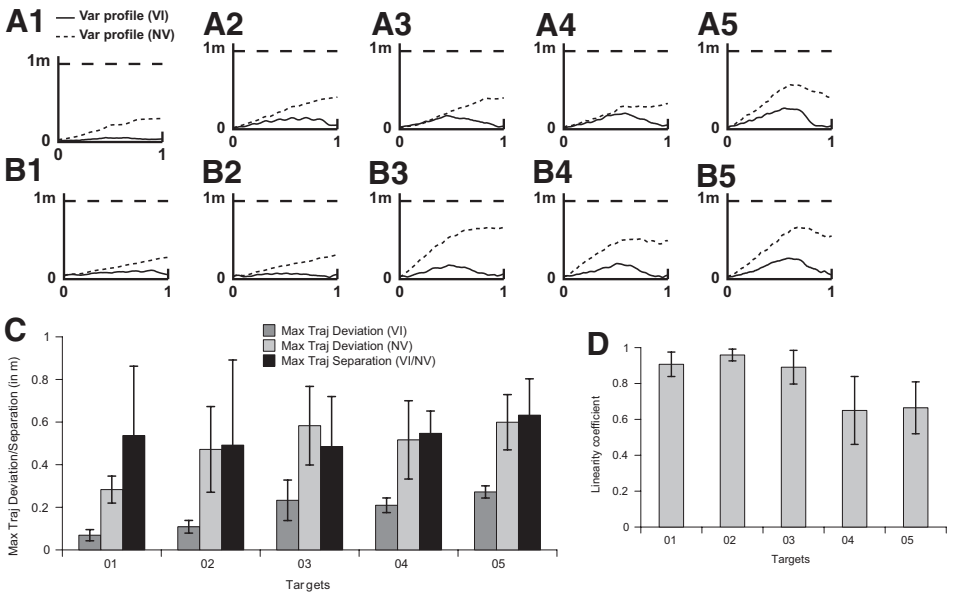

FIG. 4. *Experiment* 2: comparison of variability profiles in the VI (plain lines) and NV (dashed lines) conditions. *A*: variability profiles for *subject LH*. *A1*: target 1 . *A5*: target 5. *B*: same as in *A* but for *subject NV*. *C*: average MTD across targets in condition VI (dark gray bars) and in condition NV (light gray bars), average MTS across targets between conditions VI and NV (black bars). Here the MTD and MTS were computed in an intrasubject fashion. First, for each subject, a MTD (or MTS) was computed over the 8 trials corresponding to this subject, then the average values and SDs of the MTD (or MTS) across the 5 subjects were plotted. *D*: linearity coefficients LC ($0 \leq L C \leq 1$ and LC = 1 for a linear function, see METHODS).

4, *A, 1* and *2,* and *B, 1* and *2*), whereas for the latter, the variability was higher around the middle of the movement than around the ends, yielding a *"bump-shape" variability profile* (*A, 3–5,* and *B, 3–5*).

SPECIAL SHAPES OF THE VARIABILITY PROFILES IN NONVISUAL LOCOMOTION (*EXPERIMENT 2*). In condition NV, the variability did not decrease toward zero at the end of the movement as in condition VI. For the straight targets (targets 1 and 2), the variability increased approximately linearly with time so that the variability profiles could be approximated by a straight line (Fig. 4, *A, 1* and *2,* and *B, 1* and *2,* dashed lines). This was confirmed by the calculation of the average LC across subjects, which were close to 1 for these targets (Fig. 4*D*).

For the most angled targets (targets 4 and 5), the variability profiles were not linear: the average LC across subjects was ~0.65 for these targets. Indeed the variability profiles corresponding to these targets were clearly composed of two parts: a first part where the variability increased linearly and a second part where the variability remained constant (see the dashed lines in Fig. 4, *A4* and *B4*) or even decreased (*A5* and *B5*). We propose in *Variability around the average trajectory* a hypothesis accounting for this interesting property.

WALKING SPEED AFFECTS NEITHER THE AVERAGE TRAJECTORIES NOR THE VARIABILITY PROFILES (*EXPERIMENT 3*). The speed instruction was well respected: subjects did walk faster in condition FS than in condition NS. The average speed across targets, subjects and trials was 1.34 ± 0.11 m/s in condition NS and 1.60 ± 0.16 m/s in condition FS. From condition NS to FS, the subjects increased their speed by between 13 and 30%. In the two-way ANOVA test where the factors were the speed condition and the target, the main effect of the speed condition was significant [$F(1,40) = 55.1$, $P < 0.05$], and there was no significant interaction effect [$F(4,40) = 0.09$, $P > 0.05$].

The average trajectories were also similar in the two speed conditions (Fig. 5*C*). The average $MTS_{NS/FS}$ computed across targets and subjects was 0.18 ± 0.06 m, whereas the average MTD_{NS} was 0.18 ± 0.08 m. In the two-way ANOVA test where the factors were the speed condition and the target, the main effect of the speed condition was not significant [$F(1,40) = 0.01$, $P > 0.05$]. However, the interaction effect was significant [$F(4,40) = 5.7$, $P < 0.05$]. In other words, the difference between the average trajectories in the two conditions was globally of the same magnitude as the variability within condition NS, but target-wise, there were differences between $MTS_{NS/FS}$ and MTD_{NS}. However, for the most interesting targets (targets 4 and 5), we found that $MTS_{NS/FS} < MTD_{NS}$ (Fig. 5*C*).

The variability profiles measured in the two speed conditions were very similar, in terms of both shape and magnitude (see Fig. 5, *A* and *B,* for typical variability profiles). For the straight targets, the variability was low throughout the movement, and for the angled targets, bump-shaped variability profiles were consistently observed in both speed conditions. In the two-way ANOVA test where the factors were the speed condition and the target, the main effect of speed condition on the MTDs was not significant [$F(1,40) = 0.006$, $P > 0.05$], neither was the interaction effect [$F(4,40) = 1.2$, $P > 0.05$].

PRESENCE OF VIA-POINTS AFFECTS THE VARIABILITY PROFILES (*EXPERIMENT 4*). We noted first that the average trajectories recorded in the three sessions were very similar, as we could expect from the experimental setup. For instance, the MTS between the average trajectory of session 1 (no-via-point) and that of session 2 (1-via-point) was 0.12 ± 0.07 m. Similarly, the MTS between the average trajectory of session 1 (no-via-point) and that of session 3 (3-via-points) was 0.11 ± 0.06 m.

Consistently with the previous results, the variability profiles observed in the no-via-point condition were bump-shaped (Fig. 6, *A1* and *B*). By contrast, the variability profiles in the 1-via-point condition were clearly two-peaked with a local minimum occurring around $t = 0.5$ (Fig. 6, *A2* and *B*). The variability profiles in the 3-via-points condition displayed smaller variations than in the two previous conditions. In particular, we observed no significant peaks or valleys (Fig. 6*A3* and *B*).

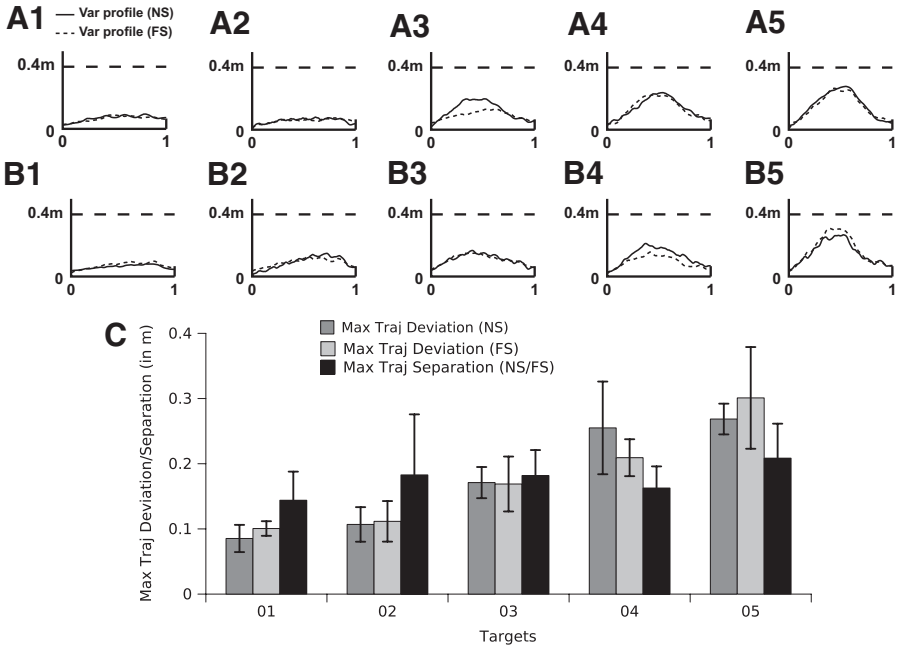

FIG. 5. *Experiment* 3: comparison of variability profiles in the normal speed (NS: plain lines) and fast speed (FS: dashed lines) conditions. For details, see legend of Fig. 4. *A*: variability profiles for *subject B. B*: same as in *A* but for *subject RK. C*: average MTD across targets in condition NS (dark gray bars) and in condition FS (light gray bars), average MTS across targets between conditions NS and FS (black bars).

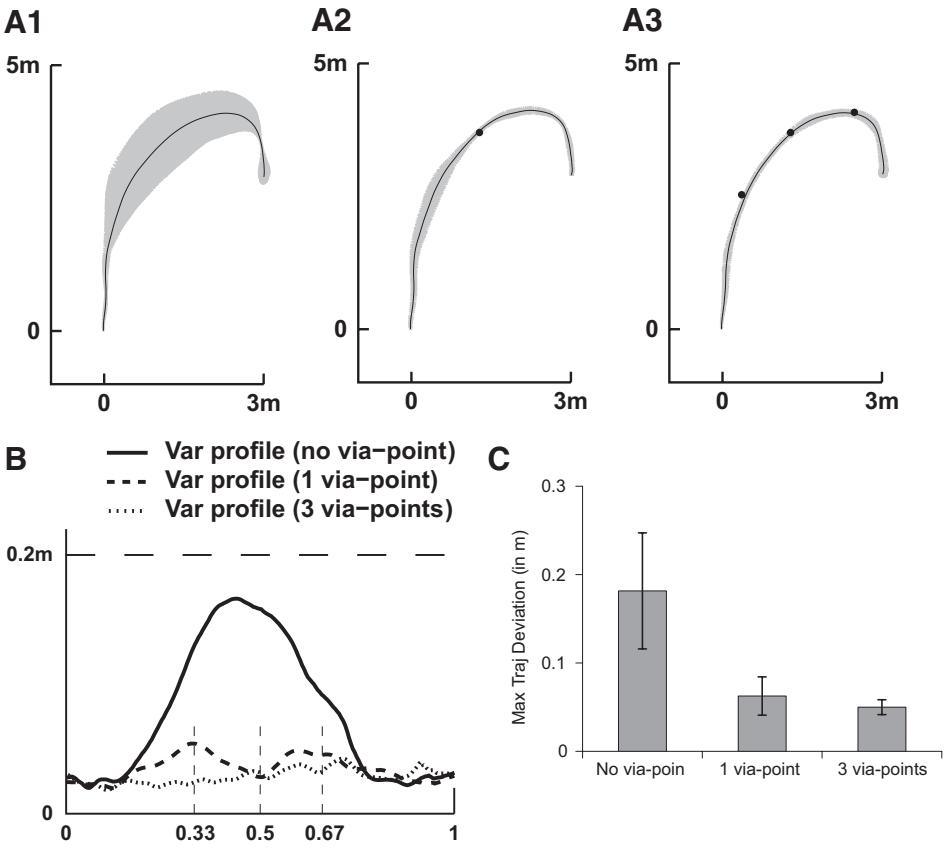

FIG. 6. *Experiment 4*: testing the desired-trajectory hypothesis. *A*: average trajectories and variance ellipses around the average trajectories. *A1*: no-via-point condition. *A2*: 1-via-point condition. *A3*: 3-via-points condition. *B*: average variability profiles computed across subjects. —, no via point; - - -, 1 via point; ···, 3 via points. We also indicated the time instants $t = 0.33$, $t = 0.5$, and $t = 0.67$ for which the via points where computed. *C*: average MTD across subjects in the 3 conditions.

Quantitatively, the MTD in the 1-via-point (0.06 ± 0.02 m) and the 3-via-points (0.05 ± 0.008 m) conditions were lower than the MTD in the no-via-point condition (0.18 ± 0.06 m). The one-way ANOVA test revealed that the number of via points (0, 1, or 3) has a significant effect on the MTDs [$F(2,12) = 16.3$, $P < 0.05$]. The post hoc Tukey tests revealed that this effect was significant between the 0- and 1-via-point conditions and between the 0- and 3 via-points conditions but not between the 1- and 3-via-points conditions.

Variability around the average trajectory: combination of two independent components

HYPOTHESIS ON THE STRUCTURE OF THE VARIABILITY PROFILES. We propose to study now in more detail the *structure* of the variability profiles observed in the nonvisual condition, based on the results of *experiment 2*. In this experiment, two parameters were varied: the presence or absence of visual feedbacks and the "complexity" of the target; that is, specifically, whether the target was "straight" or "angled." We make the hypothesis that these two parameters *independently contribute* to the variability profiles.

More precisely, our hypothesis states that the variability recorded for the different targets and visual conditions results from the combination of the variabilities produced by two mutually independent sources. The first source is vision-dependent and "trajectory complexity"-independent: that is, independent of whether the target is straight or angled. The second source is trajectory complexity-dependent and vision-independent. The psychological and physiological interpretations of these two sources are addressed in the DISCUSSION.

The variability resulting from source 1—which is trajectory complexity-independent—can be isolated by examining the trials involving only straight targets: indeed, for these "easy" trials, the contribution of source 2—which is trajectory complexity-dependent—should be minimal. Now from the results of *experiment 2,* we know that the variability in question is almost zero in the visual condition and that it increases approximately linearly with time in the nonvisual condition. Similarly, the variability resulting from source 2—which is vision-independent—can be isolated by examining the trials executed with vision. For the straight targets, this variability is almost zero, whereas for the angled targets, this variability describes, as a function of time, the shape of a bump (see RESULTS of *experiment 2* in the preceding text).

OBSERVATION SUPPORTING THE HYPOTHESIS. The proposed "two-sources" hypothesis allows now to make the following nontrivial observation: the special shape of the variability profiles observed in condition NV for the angled targets can be decomposed as the sum of a *straight line* (source 1) and of a *bump profile* (source 2): see Table 1 for a summary.

TABLE 1. *The two-sources hypothesis*

Visual Condition/Target	Straight Targets	Angled Targets
Visual	0 + 0	0 + Bump
Nonvisual	Line + 0	Line + Bump

In each cell, we indicate the putative contribution of source 1 (vision-dependent, "trajectory-complexity"-independent) + the putative contribution of source 2 (vision-independent, "trajectory-complexity" dependent).

To illustrate this, let us denote by TD^n_{VI} and TD^n_{NV} the variability profiles corresponding to target n in condition VI and condition NV, respectively. The preceding observation implies that TD^n_{NV} would be similar to the sum of the *bump-shaped variability profile* observed for the same target in condition VI (TD^n_{VI}), plus a *straight-line variability profile* (for simplicity, we chose the variability profile corresponding to target 2: TD^2_{NV}).

Figure 7A shows the comparison of TD^4_{NV} with the sum $TD^4_{VI} + TD^2_{NV}$ for the five tested subjects of *experiment 2*. Similarly, Fig. 7*B* shows the comparison of TD^5_{NV} with the sum $TD^5_{VI} + TD^2_{NV}$. One can observe in each case a good match between the compared profiles.

However, this observation should not be taken literally. While the proposed hypothesis concerns the noise *sources*, we compared above the *trajectory variabilities*, that is, the *output* of the whole trajectory generation process. In this respect, it should be noted that, whenever the trajectory generation mechanisms contain nonlinearities, the additivity of the two noise sources would not translate into the additivity of the trajectory variability profiles. Following this remark, we did not seek to find the best combination of the two *squared* variability profiles (indeed, the variability profiles were given by the 2D SDs of the trajectories, but for linear systems only *variances* add up). We chose instead to show directly the sum of the variability profiles as a way to hint how the special shapes of the variability profiles observed in *experiment 2* can be obtained from the combination of a line and a bump profile. To assess the hypothesis in a more formal way, it is necessary to evaluate the input-output relationship between the incoming noise and the resulting trajectory variability. This is addressed in the modeling study where we propose a possible *implementation* of the trajectory generation mechanism.

MODELING STUDY

While integrating the previous experimental findings within a unifying framework, the following modeling study also allows testing *positively formulated* control mechanisms. In particular, we propose that the on-line control of whole-body trajectories in visual *and* nonvisual locomotion may be based on optimal feedback control. To test this idea, we designed a simplified optimal feedback control model and compared the predictions of this model (and those of alternative models) with

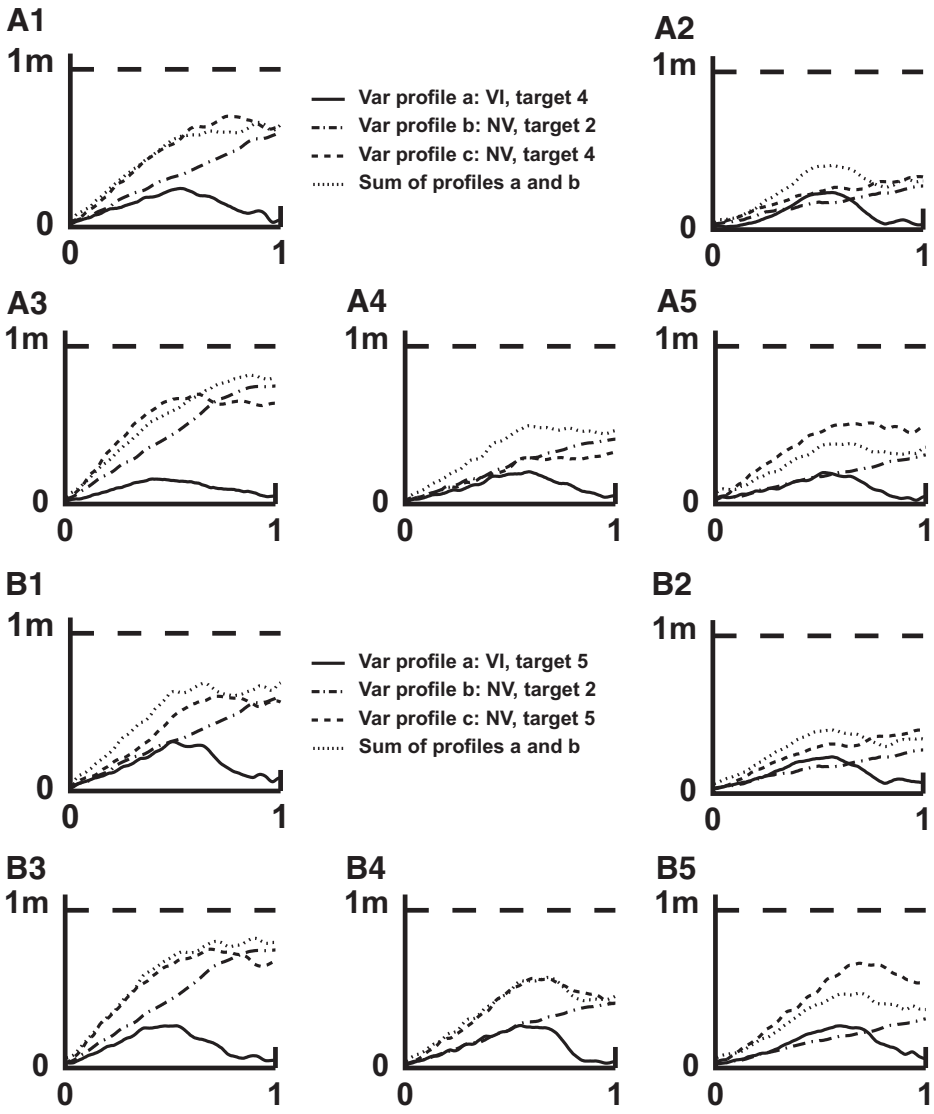

FIG. 7. Testing the 2-sources hypothesis. *A*: variability profiles for target 4 and *subjects AN* (*A1*), *DP* (*A2*), *GN* (*A3*), *LH* (*A4*), and *NV* (*A5*). —, variability profile for target 4 in condition VI; -·-, variability profile for target 2 in condition NV. Compare - - - (variability profile for target 4 in condition NV) with ··· (sum of the — and the -·-). *B*: same legend as in *A* but for target 5.

the experimentally recorded trajectories. Furthermore, as stated previously, the model allows formally testing whether the combination of the two sources (vision-independent and trajectory-complexity-independent) could give rise to the special shape of the variability profiles observed in *experiment 2*.

We first describe a modified version of the minimum jerk model on which our optimal feedback control model is based.

Deterministic modified minimum jerk (MMJ) model

DESCRIPTION *OF THE MODEL.* In (Pham et al. 2007), we presented a minimum jerk model (Flash and Hogan 1985) that could reproduce with great accuracy locomotor trajectories of moderate curvature. However, we noticed that the original minimum jerk model predicted velocity profiles that displayed slightly larger variations than those experimentally observed. For this reason, the simple minimum jerk model failed to predict trajectories recorded in the present experiments, which were highly curved.

To overcome this, we added an extra term that penalizes large variations of the velocity. The influence of this term is weighted by a constant γ that we set to a unique value ($\gamma = 1{,}000$) in all the simulations for genericity. Thus we looked for the trajectory $[x(t), y(t)]$, $0 \leq t \leq 1$ that minimizes

$$\int_0^1 \dddot{x}^2 + \dddot{y}^2 + \gamma \left(\frac{d}{dt} \sqrt{\dot{x}^2 + \dot{y}^2} \right)^2 dt \qquad (12)$$

subject to the constraints

$$\begin{aligned} &x(0) = x_0;\ \dot{x}(0) = v_0^x;\ \ddot{x}(0) = a_0^x;\ x(1) = x_1;\ \dot{x}(1) = v_1^x;\ \ddot{x}(1) = a_1^x \\ &y(0) = y_0;\ \dot{y}(0) = v_0^y;\ \ddot{y}(0) = a_0^y;\ y(1) = y_1;\ \dot{y}(1) = v_1^y;\ \ddot{y}(1) = a_1^y \end{aligned} \qquad (13)$$

where the 12 boundary conditions (x_0, $v^x{}_0$, $a^x{}_0$, . . .) were set to the respective average experimental values. We found approximated solutions by numerically solving this optimization problem in the subspace of polynomials of degrees ≤ 7 (see Pham et al. 2007 for more details).

Performance of the model

To assess the quality of the model's prediction, we defined the instantaneous trajectory error (TE) of model M ($M = j$ for the original minimum jerk model and $M = m$ for the modified minimum jerk model) by

$$\mathrm{TE}_M(t) = \sqrt{[x_M(t) - x_{av}(t)]^2 + [y_M(t) - y_{av}(t)]^2} \qquad (14)$$

where $[x_{av}(t), y_{av}(t)]$ is the experimentally recorded average trajectory and $([x_M(t), y_M(t)]$ is the trajectory predicted by the model. The maximal trajectory error (MTE) was defined by

$$\mathrm{MTE}_M = \max_{0 \leq t \leq 1} \mathrm{TE}_M(t) \qquad (15)$$

We compared, for the targets of *experiment 1,* the average trajectories measured in condition VI with the predicted trajectories. For clarity, we divided the targets into two groups: group I containing straight and moderately angled targets (1N, 2N, 3N, 4N, 5N, 4E, 5E) and group II containing highly angled targets (4W, 5W, 4S, 5S). One-way ANOVA tests with replications were then performed to compare the MTD of the trajectories recorded in condition VI with the MTE of the models (3 levels: MTD, $\mathrm{MTE_j}$, $\mathrm{MTE_m}$). If a significant effect was found, we performed post hoc Tukey tests to compare between each pair.

Result: the modified minimum jerk can accurately predict the average trajectories for a wide range of targets

For the straight and moderately angled targets (group I: targets 1N, 2N, 3N, 4N, 5N, 4E, 5E), the original and the modified minimum jerk models yielded accurate predictions, in terms of both trajectory path (Fig. 8*A1*) and velocity profile (*A2*). The average $\mathrm{MTE_j}$ across the targets of group I was 0.11 m, and the average $\mathrm{MTE_m}$ was <0.14 m, while the average MTD was 0.26 m. The difference among the three means was significant [$F(2,18) = 10.2$, $P < 0.05$]. The post hoc Tukey tests revealed that the difference between MTD and $\mathrm{MTE_j}$ and the difference between MTD and $\mathrm{MTE_m}$ were significant, whereas the difference between $\mathrm{MTE_j}$ and $\mathrm{MTE_m}$ was not. The last result can be explained by the fact that, because the magnitude of the variations in the velocity profiles predicted by the original model were not too large, the addition of the extra term in the objective function did not affect the predicted trajectories (Fig. 8*A, 1* and *2*).

By contrast, for the highly angled targets (group II: targets 4W, 5W, 4S, 5S, see Fig. 8, *B2* and *C2*), the velocity profiles predicted by the original minimum jerk model showed very large fluctuations. This resulted in a larger dissimilarity between the predicted and the experimentally recorded trajectories, in terms of both velocity profile (Fig. 8, *B2* and *C2*) and trajectory path (*B1* and *C1*). Quantitatively, the average $\mathrm{MTE_j}$ across the targets of group II was 0.54 m, the average $\mathrm{MTE_m}$ was 0.29 m, whereas the average MTD was 0.40 m. The difference among the three means was significant [$F(2,9) = 7.7$, $P < 0.05$]. The post hoc Tukey tests revealed that the difference between $\mathrm{MTE_j}$ and $\mathrm{MTE_m}$ was significant, meaning that the modified minimum jerk does significantly better than the original model. Indeed the addition of the extra term effectively reduced the variations of the speed, so that the velocity profiles predicted by the modified model very closely resembled the experimentally observed ones (Fig. 8, *B2* and *C2*). In terms of trajectory paths, the modified model also "bent" the minimum jerk paths toward the experimentally observed paths, although no "instruction" about the path was specified in this model.

Stochastic models

VISUAL (VI) CONDITION. The model given by algorithm 1 implements a *simplified optimal feedback control* scheme (Hoff and Arbib 1993; Todorov and Jordan 2002). Following the experimental results, this model relies on an open-loop process that is complemented by an on-line feedback module (see Figs. 1 and 9*A* for illustrations). The open-loop process is based on the maximum-smoothness principle (see preceding text), whereas the feedback module is based on the optimal feedback control principle.

Algorithm 1 (see Fig. 9A for illustration)

1) Discretize the movement into n steps ($10 \leq n \leq 20$ depending on the target).

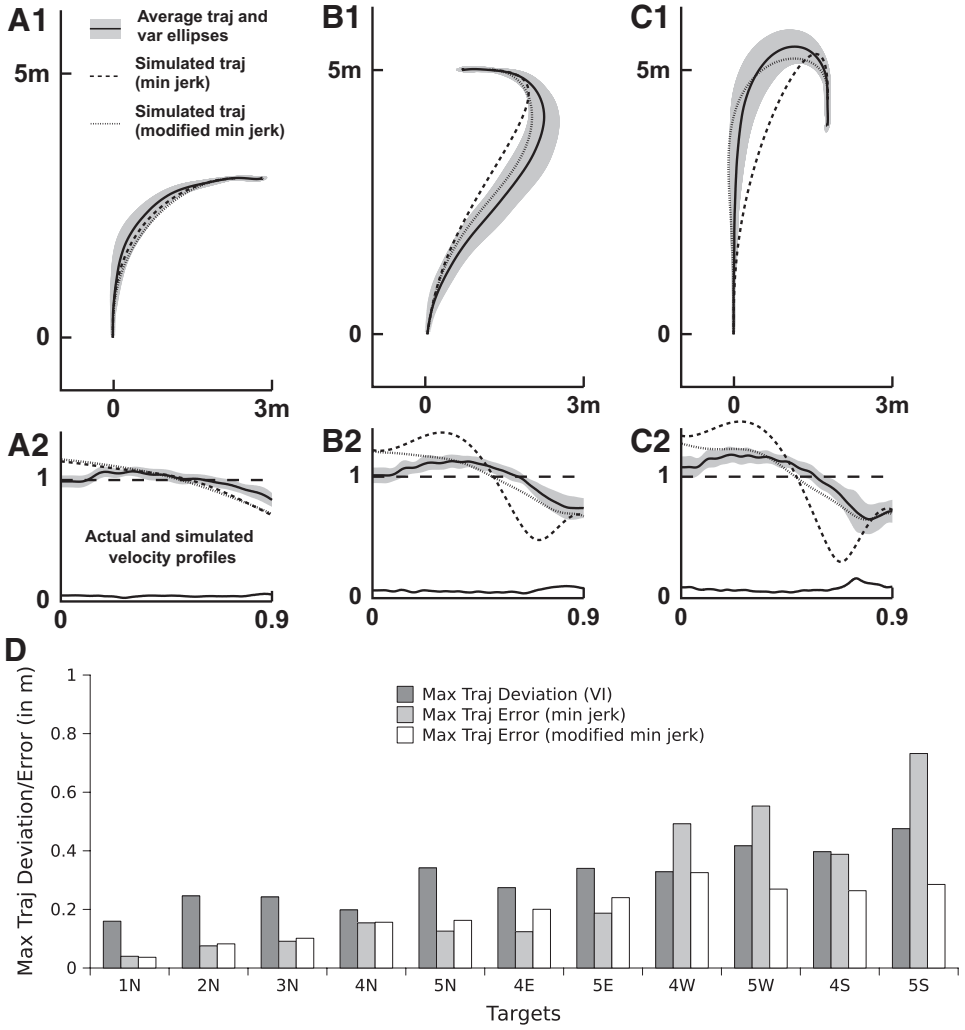

FIG. 8. Modeling results for the deterministic modified minimum jerk model. *A*: modeling results for target 4E. *A1*: geometric path of the average trajectory (plain line) and variance ellipses around the average trajectory (gray area), geometric path of the trajectory predicted by the original minimum jerk model (dashed line) and by the modified minimum jerk model (dotted line). *A2*: average normalized velocity profile (plain line), normalized velocity profiles predicted by the original minimum jerk model (dashed line) and by the modified minimum jerk model (dotted line). The normalization was done so that the mean normalized velocity over the whole trajectory equals 1 (see METHODS and also Pham et al. 2007). (*B*) Same as in *A* but for target 5W. *C*: same as in *A* but for target 5S. *D*: MTD in condition VI (dark gray bars), maximal trajectory error (MTE) for the original minimum jerk model (light gray bars), MTE for the modified minimum jerk model (white bars).

2) At each step i, compute first a MMJ trajectory between the current state $s(i)$ (position, velocity, acceleration at time step i) and the final state. This is the initially planned trajectory.

3) Add a random perturbation to $s'(i + 1)$, the state of the initially planned trajectory at step $i + 1$. This yields the actual state $s(i + 1)$.

4) Interpolate a smooth trajectory between $s(i)$ and $s(i + 1)$ (for simplicity, we used a MJ trajectory because it is the lowest-order polynomial trajectory T that satisfy $T(0) = s(i)$ and $T(1) = s(i + 1)$: see APPENDIX in Pham et al. 2007 and references therein). This yields the actual sub-trajectory between i and $i + 1$.

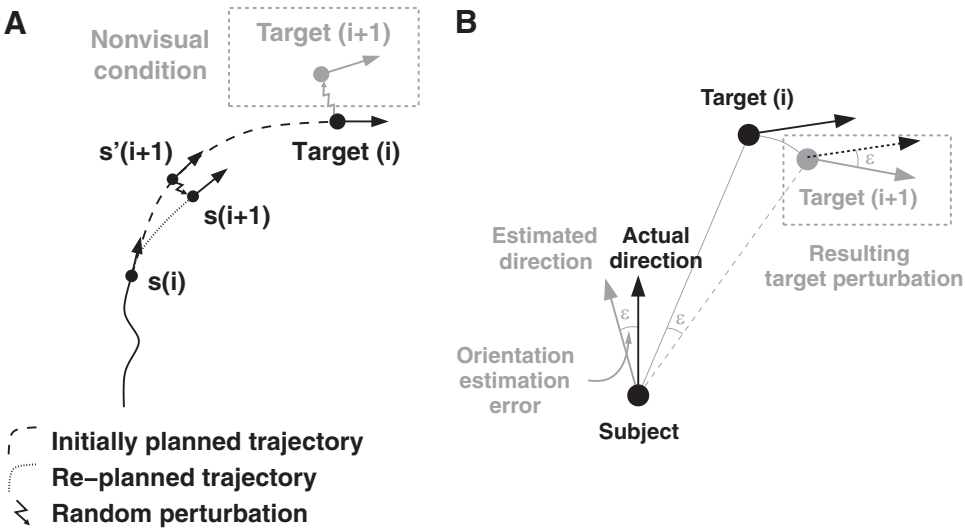

FIG. 9. Illustration for the simplified optimal feedback control models. *A*: illustration for algorithm 1 and for its modified version (NV condition). *B*: effect of an error in the subject's estimation of his orientation in space.

5) Repeat from step 2.

We note that this model is a not a fully optimal feedback control model in the sense of Todorov and Jordan (2002) because in the step where we computed the $(i + 1)^{th}$ optimal subtrajectory (step 2 of algorithm 1), we minimized the deterministic cost instead of the "cost-to-go" (which also takes into account the statistics of the noise) (see Todorov and Jordan 2002). However, this model preserves the main idea of optimal feedback control, namely, that the subtrajectories are recomputed at every step optimally with respect to the final target and not with respect to any intermediate representation of the task (such as a "desired trajectory").

The initial and final velocities and accelerations in algorithm 1 were set to the average experimental values as in the deterministic model. To reproduce the small baseline variability present at the beginning and at the end of the movement, the initial and final positions were chosen from a 2D Gaussian distribution with SD ($\sigma^x_{\text{baseline}} = 0.027$ m; $\sigma\sigma^y_{\text{baseline}} = 0.027$ m) and centered around the actual starting position and the actual target's position.

Regarding the perturbations added at step 3 of the algorithm, Harris and Wolpert (1998) argued that the amount of execution noise (see DISCUSSION) is likely an increasing function of the "motor commands." However, because we did not model directly the whole locomotor apparatus but only its outcome (the locomotor trajectory), it is unclear how execution noise may be "converted" into trajectory perturbations. Here, in the context of locomotion, a series of observations suggest that the magnitude of the trajectory perturbations caused by execution noise is likely determined by the instantaneous trajectory curvature and not by, for instance, velocity or acceleration. First, trajectory variability was higher for the angled targets, which impose curved trajectories, than for the straight targets (*experiments 1* and *2*). This rules out velocity as a determining factor, because velocity was usually lower for curved trajectories. Second, the variability profiles were the same in the NS and FS conditions (*experiment 3*) although the kinematic quantities, such as velocity or acceleration, were larger in condition FS than in condition NS. By contrast, the observed geometric paths (hence the curvature distributions) were the same in the two conditions.

We thus set the magnitude of the trajectories perturbations to be an increasing affine function (van Beers et al. 2004) of the absolute value of the curvature (in a different context, the absolute value of the curvature was used in a model of locomotor trajectories formation) (see Arechavaleta et al. 2008). The total trajectory perturbation is then the sum of a constant perturbation and a signal-dependent perturbation that scales linearly with the absolute value of the curvature

$$\sigma^x_{\text{exec}}(t) = \sigma^y_{\text{exec}}(t) = \sigma_{\text{const}} + |\kappa(t)|\sigma_{\text{sd}} \quad (16)$$

where $\sigma_{\text{const}} = 0.03$ m and $\sigma_{\text{sd}} = 0.14$ m^2 for all targets.

Finally, it should be noted that our method of adding noise directly to the states (and not to the commands) constitutes a simplification. A more rigorous version of our model would require reformulating the MMJ optimization into a dynamical model, as Hoff and Arbib (1993) did for the original MJ optimization. However, in our case, the addition of the γ term in the MMJ made such a reformulation much more difficult.

NV CONDITION. To understand the variability patterns observed in condition NV, we evaluate two competing control schemes: a purely open-loop control scheme and an on-line feedback control scheme with state estimation errors.

Purely open-loop control (models OL). Here we model three possible purely open-loop control schemes, which are specified in terms of the time series of velocity, acceleration, or jerk.

We computed first the deterministic MMJ trajectory between the initial and final states (see preceding text). We then computed, by successive differentiations, three 2D time series $[v_x(i),v_y(i)]$, $[a_x(i),a_y(i)]$, and $[j_x(i),j_y(i)]$, representing respectively the velocity, acceleration and jerk profiles corresponding to this MMJ trajectory.

In model OL_v, we added Gaussian random perturbations with SD $\sigma_v(i)$ to $v_x(i)$ and $v_y(i)$ ($i = 1,\ldots,N$) to obtain a random time series $[v^*_x(i),v^*_y(i)]$. Note that $\sigma_v(i)$ was also an affine function of the instantaneous trajectory absolute curvature (the coefficients were the same as in the preceding text, but appropriately rescaled to match the experimental variability at $t = 1$). The time series $[v^*_x(i),v^*_y(i)]$ was finally integrated with respect to time to yield a random trajectory.

In models OL_a (respectively, OL_j), instead of adding the perturbation to the velocity vectors, we added Gaussian random perturbations with SD $\sigma_a(i)$ [respectively, $\sigma_j(i)$] to the acceleration (respectively, jerk) vectors. These random vectors were then integrated twice (respectively, 3 times) to yield a random trajectory.

On-line feedback control (model OF). This model was based on the simplified optimal feedback control model used for condition VI (algorithm 1). Remark first that in the VI model, the subject's state $s(i)$ (position, velocity, acceleration) was assumed to be perfectly known to the subject at every time step. To model the absence of vision in condition NV, we introduced perturbations in the subject's estimation of his state. For simplicity, we assumed that these perturbations yielded errors in terms of subject's estimated orientation and distance to target [the reduction of the state to the pair (distance, orientation) is rather classical in studies of nonvisual locomotion] (see for instance Glasauer et al. 2002; Loomis et al. 1993). Remark now that from a *computational* viewpoint, these errors can be rendered, in our model, by perturbing directly the target's orientation and position in space [however, in relation with the discussion on egocentric and allocentric strategies for navigation (Burgess et al. 2002), it should be noted that the *physiological* mechanisms underlying the errors in the estimation of self's state and of the target's state may completely differ].

To make this clear, consider for instance that the subject makes an error ε in the estimation of his orientation. This is equivalent to assume that he actually makes *no error* in the estimation of his orientation but that the subjects' estimation of the "external world" is rotated by an angle $-\varepsilon$ around the subject. Because the external world in our model comprised only the target, this corresponds to the following perturbations of the target: a rotation centered on the subject and of angle $-\varepsilon$ of the target's position and a shift of $-\varepsilon$ of the target's angle (see Fig. 9*B*). Similarly, an error δ in the subject's estimation of his distance to the target corresponds

to a translation of the external world by -δ along the subject-target axis.

More specifically, we modified algorithm 1 by adding, between steps 4 and 5, the following step "4b".

Modification of Algorithm 1 for condition NV (see Fig. 9, A *and* B, *for illustration)*

1) Draw a random distance δ from a Gaussian distribution of mean 0 and of SD σ_δ ($\sigma_\delta = 0.03$ m in the simulations). Shift the target's position by -δ along the subject-target axis.

2) Draw a random angle ε from a Gaussian distribution of mean 0 and of SD σ_ε ($\sigma_\varepsilon = 1.8^\circ$ in the simulations). Rotate the target's position by -ε around the subject. Shift the required final velocity ($v_1{}^x$, $v_1{}^y$) and acceleration ($a_1{}^x$, $a_1{}^y$) angle by -ε.

There exist several other possibilities to model the absence of vision. One can for instance add an extra 2D-Gaussian perturbation to the target's position at each time step to simulate the spatial memory decay. One can set σ_δ and σ_ε as functions of the execution noise intensity. The estimation process can also be more complex, for instance, combining optimally vestibular and proprioceptive measurements with internal predictions (see the state estimation literature for hand movements reviewed in e.g., Jordan and Wolpert 1999). However, we chose to follow the simple approach above in this first modeling study. It will be necessary in future works to design new experiments and refine this part of the model to study in detail the effects and the interactions of spatial memory decay and of the different sensory signals (e.g., visual, vestibular and proprioceptive) on the variability of nonvisual trajectories.

Result: plausibility of optimal feedback control

In condition VI, the sample trajectories predicted by the optimal feedback control model were globally similar to the trajectories observed in one typical subject (Fig. 10*A*). The variability profiles produced by the model also reproduced the typical features of actual variability profiles, namely: low and approximately constant profile for the straight targets (target 2: Fig. 10*B1*) and bump-shaped profile for the angled targets (target 5: *B2*).

In condition NV, the sample trajectories predicted by model OF (on-line feedback control) were also globally similar to the trajectories observed in one typical subject (Fig. 10*C*). Regarding the variability profiles, for the straight targets, the sample variability profile produced by model OF has the form of a straight sigmoid, which was very close to a straight line (dashed line, Fig. 10*D1*). For the angled targets, the sample variability profile produced by model OF increased approximately linearly until $t = 0.8$ and then slightly decreased (dashed line, Fig. 10*D2*).

By contrast, this nonmonotonicity, which is a characteristic property of actual variability profiles (see the results of *experiment 2*), could not be reproduced by none of the OL (purely open-loop) Models. Indeed in all of these models, the variability profiles were always increasing (OL_v: dashed-triply-dotted, OL_a: dashed-dotted, OL_j: dotted lines, Fig. 10*D2*).

DISCUSSION

Visual and nonvisual locomotion share the same open-loop process

Our experimental observations first showed that to reach a distant target, subjects produced very similar average trajectories in the VI and NV conditions. If we consider only the *final part* rather than the entire trajectory, this finding implies that the average final position and final walking direction in condition NV are close to those in condition VI, which in turn correspond to the target's position and orientation because in condition VI, the task's final constraints were well respected. In earlier studies of nonvisual locomotion (see for instance Loomis et al. 1992; Thomson 1983), it was also reported that in a task where the subject had to walk without visual feedbacks to a previously seen targets, the average final position of

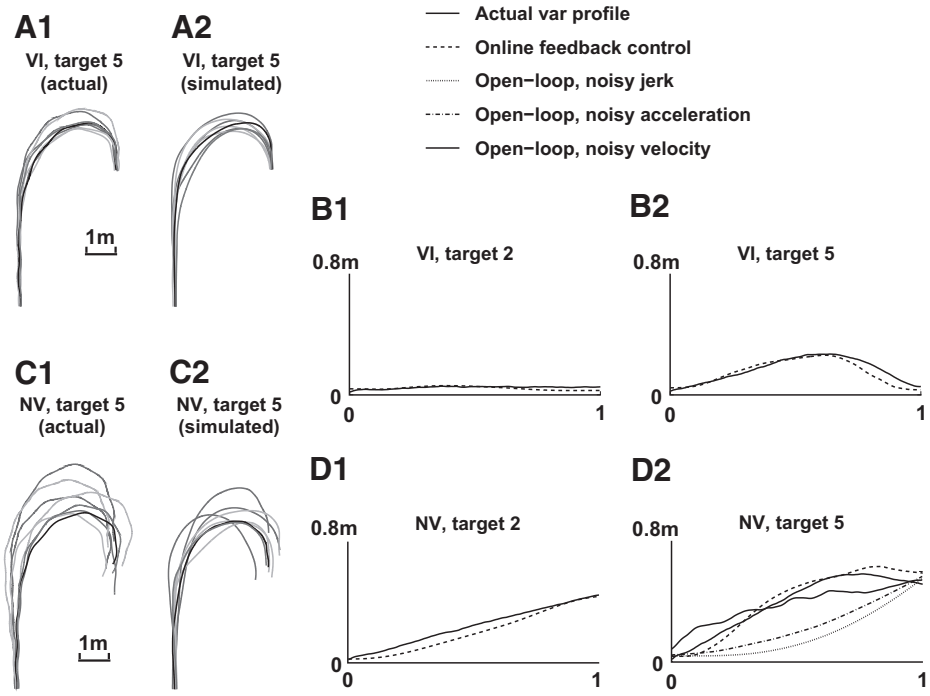

FIG. 10. Modeling results for the stochastic models. *A*: trajectories in the VI condition. *A1*: 8 actual trajectories of *subject NV* for target 5. *A2*: 8 sample trajectories simulated by the stochastic model for target 5. *B*: variability profiles in condition VI. *B1*: variability profiles for target 2. —: average variability profile across subjects. - - -: variability profile computed over 20 simulated trajectories. *B2*: same as in *B1* but for target 5. *C*: trajectories in the NV condition. *C1*: 8 actual trajectories of *subject NV* for target 5. *C2*: 8 sample trajectories simulated by model OF (stochastic MMJ + state estimation error) for target 5. *D*: variability profiles in condition NV. *D1*: variability profiles for target 2. —: average variability profile across subjects. - - -: variability profile computed over 20 sample trajectories (model OF). *D2*: variability profiles for target 5. —: average variability profile across subjects. - - -: variability profile computed over 20 sample trajectories (model OF). -···-: model OL_v (open-loop control, noisy velocity). -···-. Model OL_a (open-loop, noisy acceleration). ···: model OL_j (open-loop, noisy jerk).

the subject almost coincides with the actual position of the target. This precise average response was interpreted as reflecting the veridicality of the subjects' visual space perception (see Loomis et al. 1992). However, in these studies, the targets consisted of spots placed at various distances *in front* of the subject. Using targets defined in both position and orientation and placed at various off-axis positions, our study confirms and generalizes the earlier results mentioned in the preceding text. It also suggests that the notion of visual space perception veridicality may not be limited to straight-ahead distances but may be also valid for the perception of off-axis distances and of changes in the body orientation.

But more importantly, not only the average final positions and orientations were similar in the VI and NV conditions, but also the *entire average trajectories* that the subjects had to produce to reach these positions and orientations. Because the average trajectory is obtained by indeed "averaging out" all the fluctuations, it reflects the open-loop process that governs the subject's movements in absence of perturbations (Todorov and Jordan 2002). Thus the similarity of the average trajectories implies that the control mechanisms in visual and nonvisual locomotion share a common *open-loop process*. This idea may have a deep theoretical implication. Indeed a number of neuroscientists believe that our representation of the space is strongly related to our movements (see for instance Berthoz and Petit 2006), a notion that can be summarized by the following statement of the great French mathematician Henri Poincaré: "To localize an object in space is to build a representation of the movements one has to make to reach it" (Poincaré 1902; chapter 4). Following this line of thinking, the proposed common open-loop process may represent the physiological basis of the psychological notion of veridicality of visual space perception.

In a recent article, Fajen and Warren (2003) challenged the very existence of an open-loop process in the control of locomotion. Based on a simulation study where the targets were modeled by attractors, the obstacles by repellers and the subject by a simple second-order dynamical system evolving in a field of attractors and repellers, these authors argued that "the [subject] adopts a particular route through the scene on the basis of local responses to visually specified [targets] and obstacles. The observed route is not determined in advance through explicit planning, but rather emerges in an on-line manner from the [subject's] interactions with the environment." It should also be remarked that these interactions, which are crucial in Fajen and Warren's approach, are fundamentally based on the availability of visual inputs. In opposition to this view, the similarity of the average trajectories in the VI and NV condition reported in the present article suggests that the formation of locomotor trajectories is not exclusively driven by vision. Rather as formalized in our experimentally-confirmed model, a combination of *open-loop* and *on-line* control mechanisms underlies goal-oriented locomotion.

In the present study, we did not address the physiology underlying the on-line control mechanisms. For instance, in condition VI, how optic-flow-based (Warren et al. 2001) or gaze-direction-based (Rushton et al. 1998) information is combined and processed in the on-line feedback module could not be answered in our study. Similarly, in condition NV, the specific contributions of vestibular and proprioceptive feedback and of efference copy/corollary discharge could not be discriminated here; this may be done through clinical studies, involving for instance patients with vestibular disorders (Glasauer et al. 2002).

Origin of the variability and nature of the control mechanisms in visual locomotion

EXECUTION NOISE IN LOCOMOTION. In contrast with the similarity of the average trajectories, we reported large differences in terms of variability profiles in conditions VI and NV. Before addressing this aspect, we first discuss in more detail the origin and nature of the variability in visual locomotion.

Within the theoretical framework of computational motor control as it has been developed for hand reaching movements, it was proposed that movement variability may arise during three processes: target localization, movement planning, and movement execution (Schmidt et al. 1979; van Beers et al. 2004). We assume here that this three-sources distinction also holds for "locomotor reaching." Given this, we argue that the variability profiles observed in the visual conditions of *experiments 2–4* mostly resulted from execution noise. Indeed regarding first the target localization process, the target was clearly visible and remained so during the whole movement. Second, because we conducted an *intrasubject* analysis, the contribution of planning variability to the overall variability was reduced: indeed, a large part of planning variability arises from differences in subjects' morphologies or personal preferences. Finally, we reason by analogy with hand movements and follow van Beers and colleagues (2004) who demonstrated that—for hand movements—"in general, execution noise account for at least a large proportion of movement variability."

In hand movements, execution noise may arise at different levels (Faisal et al. 2008; van Beers et al. 2004): motor commands (the elaboration and the transmission of the neural signals may be corrupted at any stage of the neural chain, from cortical structures to motoneurons), muscle contractions (the motor response of a muscle to a given neural signal is inherently variable), etc. Because locomotion involves the production of muscle contraction patterns (lower-body muscles for forward propulsion, but also arm and trunk muscles for stability and neck muscles for steering), execution noise can also step in at all these levels. However, because the number of muscles involved in locomotion is much larger than in hand movements, the exact relationship between whole-body trajectory variability and the muscles' execution noises is harder to establish.

As evoked in the INTRODUCTION, locomotion involves also a "navigational" aspect in addition to the purely motor aspect. Indeed, locomotion is the only motor activity in which the spatial position and orientation (in conditions other than straight-ahead locomotion) of the body and of the sensory systems change throughout movement execution. In this respect, special attention should be devoted to the references frames that are used for the perception of movement (Berthoz 1991): in contrast with the case of hand movements, these reference frames move during the locomotor task. For instance, the manipulation of changing points of view over time may introduce errors in the recovering of the heading from retinal flow. In any case, the errors in the updating of the body's position and orientation may in turn contribute to the variability of the trajectory during movement execution. Other cognitive processes, such as the

fixation of various objects in the environment (see for instance Turano et al. 2001), may also introduce perturbations at this level. To study in detail the specific contribution of the motor and "navigational" levels to execution noise, a differential analysis may be conducted, for example, by comparing the variability observed during navigation in virtual environments with that observed during real-world locomotion.

ON-LINE FEEDBACK CONTROL OF LOCOMOTION IN VISUAL LOCOMOTION. To fully explain the variability of locomotor trajectories, one has to understand not only the nature of the *noise* but also that of the *control mechanisms* at work for the form of the variability arises from the interplay between these two elements. A given noise pattern may indeed give rise to different variability profiles depending on the control scheme used by the subject.

More precisely, we have distinguished in the INTRODUCTION two families of control schemes: purely open-loop control and on-line feedback control. As already mentioned, in a purely open-loop control scheme, there are no feedback corrections during task execution. The errors can hence only *accumulate*, leading to monotonically increasing variability (see also Todorov and Jordan 2002). This observation was confirmed by the modeling study: the purely open-loop models all produced monotonically increasing variability profiles. By contrast, the results of *experiments 1–3* showed that, for the "angled" targets, the variability profiles in condition VI always increased at the beginning of the movement but then decreased toward zero at the end of the movement, yielding bump-shaped profiles. From a computational perspective, these variability profiles were well reproduced by the on-line feedback model corresponding to condition VI. Taken together, these observations indicate that on-line feedback control is present in visual locomotion. This is not surprising because in general, purely open-loop control exists only in very fast, ballistic movements such as fast hand reaching. Here, since the movements we studied lasted from 3 to 10 s, this allowed the detection of the errors and the implementation of on-line corrections if necessary.

ON THE "DESIRED TRAJECTORY" HYPOTHESIS FOR LOCOMOTION. The precise nature of the on-line feedback control cannot however be determined solely from the variability profiles recorded in *experiments 1–3*. Indeed both the "desired trajectory" hypothesis and the fully optimal control hypothesis can yield bump-shaped variability profiles in the limited conditions of these experiments. However, the results of *experiment 4* are incompatible with a basic desired trajectory control scheme. Indeed as indicated in the INTRODUCTION, the desired trajectory hypothesis implies that during the planning stage, a desired optimal trajectory is computed. Empirically, this desired trajectory can be assimilated to the average trajectory computed across a large number of trials. Then during the execution stage, a trajectory tracking mechanism is used to achieve the desired trajectory. In *experiment 4,* because the average trajectories were forced by the experimental protocol to be very similar in the three conditions (0, 1, and 3 via points), the desired trajectory hypothesis would predict practically no difference between the statistics of the trajectories performed in these conditions. Thus the large differences we reported regarding the variability profiles in the three conditions indicated that the desired trajectory hypothesis should be rejected.

We note nonetheless that the results of *experiment 4* cannot rule out a variation of the desired trajectory hypothesis, which consists of *1*) constructing *several* desired subtrajectories (2 subtrajectories in the 1-via-point condition —the 1st trajectory between the starting position and the via point, the 2nd trajectory between the via point and the final position—and 4 subtrajectories in the 3-via-points conditions) and *2*) tracking *sequentially* these subtrajectories. While this variation may seem unlikely (indeed, in postexperiment interviews, the subjects reported that they conceived the trajectory as a whole and not as a sequence of subtrajectories glued together at the via points), it cannot be theoretically ruled out. This remark also applies for the original experiment of Fig. 3 in (Todorov and Jordan 2002) which inspired our *experiment 4*.

A more likely explanation for the results of *experiment 4* involves an optimal feedback control scheme. Within this scheme, on-line corrections would be made with respect to the task goal [namely, go through the via points (if present) and reach the targets] and not with respect to any intermediate representation (e.g., a desired trajectory). In the no-via-point condition, because no other constraints than the goal was specified, random deviations away from the average trajectory were not corrected if they did not interfere with this task, allowing variability to accumulate around the middle of the trajectory, thus yielding bump-shaped variability profiles. By contrast, when via-points were imposed, the corrections were made to ensure that the trajectory go through these via-points, resulting in low variability around the via-points (see also the discussion about trajectory redundancy in Todorov and Jordan 2002).

On-line control of locomotor trajectories in nonvisual locomotion

While it is easy to conceive that on-line feedback control is present in normal visual locomotion, the fact that such a mechanism may also be present when vision is totally excluded during task execution may be more surprising. Yet we observed in *experiment 2* that the nonvisual variability profiles were not always monotonic: for "angled" targets, the variability decreased near the end of the trajectory. The same arguments as previously then imply that on-line control is also present in nonvisual locomotion.

The idea that on-line control may be present in nonvisual locomotion had been proposed earlier in the literature. For instance, in Farrell and Thomson's (1999) experiment, the subject had to walk with or without vision toward a previously seen target placed at eight paces, eight paces minus 40 cm, or eight paces plus 40 cm in front of him. He had to start with his right foot and to land on the target with his left foot. The authors showed that in both conditions, the subject *functionally* adjusts the lengths of his final steps, *on a trial-to-trial basis*, to land on the target with the specified foot.

The precise nature of that on-line control has however remained unclear. For instance, while Farrell and Thomson rightly remarked that, in the nonvisual condition, "[the subjects] adjust their step lengths in a way similar to that seen in the visual condition," they did not provide an interpretation of the nature of the processes common or specific in visual and nonvisual locomotion.

Here, the two-sources hypothesis (see *Variability around the average trajectories*), directly addressed the nature of this on-line control. Indeed we showed that the variability in the nonvisual condition results from the combination of a vision-dependent component and a trajectory-complexity-dependent component.

The first component—the contribution of which is zero in condition VI and an increasing linear function of time in condition NV—can be interpreted as resulting from the errors in the subject's estimation of his state, which, in turn, are caused by the absence of visual feedbacks. This was confirmed by the modeling study, where the perturbation of the subject's state estimation at each step could reproduce the variability profiles experimentally observed in condition NV.

The second component—the contribution of which is zero for "straight" targets and bump-shaped for "angled" targets—can be interpreted as resulting from the interplay between execution noise and optimal feedback control, as explained previously in the case of visual locomotion. The fact that this component is present also in nonvisual locomotion, under almost the same form (see also the modeling study), thus suggests that the very control mechanisms that governs visual locomotion underlie nonvisual locomotion as well.

Whether our conclusions about the control mechanisms at work during nonvisual locomotion also hold in adventitiously and congenitally blind subjects remains yet to be investigated. We believe indeed that a better understanding of the control mechanisms governing nonvisual locomotion and navigation can help develop new tools assisting visually impaired individuals in their daily activities.

ACKNOWLEDGMENTS

We are deeply grateful to A. H. Olivier and A. Crétual for help with the experiments and to A. Berthoz for thoughtful comments on an earlier version of the manuscript.

GRANTS

This work was supported in part by the Agence Nationale de la Recherche PsiRob Locanthrope project. H. Hicheur was supported in part by the Alexander von Humboldt foundation.

REFERENCES

Amorim MA, Glasauer S, Corpinot K, Berthoz A. Updating an object's orientation and location during nonvisual navigation: a comparison between two processing modes. *Percept Psychophys* 59: 404–18, 1997.

Arechavaleta G, Laumond JP, Hicheur H, Berthoz A. The non-holonomic nature of human locomotion: a modeling study. In: *Proceedings of the IEEE/RAS-EMBS International Conference on Biomedical Robots and Biomechatronics.* Pisa, Italy, 2006.

Arechavaleta G, Laumond JP, Hicheur H, Berthoz A. An optimality principle governing human walking. *IEEE Trans Robot* 24: 5–14, 2008.

Bernstein N. *The Coordination and Regulation of Movements.* Oxford, UK: Pergamon, 1967.

Berthoz A. Reference frames for the perception and control of movement. In: *Brain and Space,* edited by J. Paillard. New York: Oxford Univ. Press, 1991.

Berthoz A, Petit JL. *Phénoménologie et physiologie de l'action.* Paris: Odile Jacob, 2006.

Burgess N, Maguire EA, O'Keefe J. The human hippocampus and spatial and episodic memory. *Neuron* 35: 625–641, 2002.

Capaday C. The special nature of human walking and its neural control. *Trends Neurosci* 25: 370–376, 2002.

Faisal AA, Selen LP, Wolpert DM. Noise in the nervous system. *Nat Rev Neurosci* 9: 292–303, 2008.

Fajen BR, Warren WH. Behavioral dynamics of steering, obstacle avoidance, and route selection. *J Exp Psycho Hum Percept Perform* 29: 343–362, 2003.

Farrell MJ, Thomson JA. On-line updating of spatial information during locomotion without vision. *J Mot Behav* 31: 39–53, 1999.

Flash T, Hogan N. The coordination of arm movements: an experimentally confirmed mathematical model. *J Neurosci* 5: 1688–1703, 1985.

Glasauer S, Amorim MA, Viaud-Delmon I, Berthoz A. Differential effects of labyrinthine dysfunction on distance and direction during blindfolded walking of a triangular path. *Exp Brain Res* 145: 489–497, 2002.

Harris CM, Wolpert DM. Signal-dependent noise determines motor planning. *Nature* 394: 780–784, 1998.

Hicheur H, Glasauer S, Vieilledent S, Berthoz A. Head direction control during active locomotion in humans. In: *Head Direction Cells and the Neural Mechanisms of Spatial Orientation*, edited by Wiener SI, Taube JS. Cambridge, MA: MIT Press, 2005a, p. 383–408.

Hicheur H, Pham QC, Arechavaleta G, Laumond JP, Berthoz A. The formation of trajectories during goal-oriented locomotion in humans. I. A stereotyped behavior. *Eur J Neurosci* 26: 2376–2390, 2007.

Hicheur H, Vieilledent S, Richardson MJ, Flash T, Berthoz A. Velocity and curvature in human locomotion along complex curved paths: a comparison with hand movements. *Exp Brain Res* 162: 145–154, 2005b.

Hoff B, Arbib MA. Models of trajectory formation and temporal interaction of reach and grasp. *J Mot Behav* 25: 175–192, 1993.

Jordan MI, Wolpert DM. Computational motor control. In: *The Cognitive Neurosciences*. Cambridge, MA: The MIT Press, 1999.

Liu D, Todorov E. Evidence for the flexible sensorimotor strategies predicted by optimal feedback control. *J Neurosci* 27: 9354–9368, 2007.

Loomis JM, Da Silva JA, Fujita N, Fukusima SS. Visual space perception and visually directed action. *J Exp Psychol Hum Percept Perform* 18: 906–921, 1992.

Loomis JM, Klatzky RL, Golledge RG, Cicinelli JG, Pellegrino JW, Fry PA. Nonvisual navigation by blind and sighted: assessment of path integration ability. *J Exp Psychol Gen* 122: 73–91, 1993.

Olivier AH, Crétual A. Velocity/curvature relations along a single turn in human locomotion. *Neurosci Lett* 412: 148–153, 2007.

Pham QC, Hicheur H, Arechavaleta G, Laumond JP, Berthoz A. The formation of trajectories during goal-oriented locomotion in humans. II. A maximum smoothness model. *Eur J Neurosci* 26: 2391–2403, 2007.

Philbeck JW, Loomis JM, Beall AC. Visually perceived location is an invariant in the control of action. *Percept Psychophys* 59: 601–612, 1997.

Poincaré H. *La Science et l'Hypothèse.* Paris: Flammarion, 1902.

Rushton SK, Harris JM, Lloyd MR, Wann JP. Guidance of locomotion on foot uses perceived target location rather than optic flow. *Curr Biol* 8: 1191–1194, 1998.

Schmidt RA, Zelaznik H, Hawkins B, Frank JS, Quinn JT Jr. Motor-output variability: a theory for the accuracy of rapid motor acts. *Psychol Rev* 47: 415–451, 1979.

Thomson JA. Is continuous visual monitoring necessary in visually guided locomotion? *J Exp Psychol Hum Percept Perform* 9: 427–443, 1983.

Todorov E. Optimality principles in sensorimotor control. *Nat Neurosci* 7: 907–915, 2004.

Todorov E, Jordan MI. Optimal feedback control as a theory of motor coordination. *Nat Neurosci* 5: 1226–135, 2002.

Turano KA, Geruschat DR, Baker FH, Stahl JW, Shapiro MD. Direction of gaze while walking a simple route: persons with normal vision and persons with retinitis pigmentosa. *Optom Vis Sci* 78: 667–675, 2001.

van Beers RJ, Haggard P, Wolpert DM. The role of execution noise in movement variability. *J Neurophysiol* 91: 1050–1063, 2004.

Vieilledent S, Kerlirzin Y, Dalbera S, Berthoz A. Relationship between velocity and curvature of a human locomotor trajectory. *Neurosci Lett* 305: 65–69, 2001.

Warren WH Jr, Kay BA, Zosh WD, Duchon AP, Sahuc S. Optic flow is used to control human walking. *Nat Neurosci* 4: 213–216, 2001.

Winter DA, Eng P. Kinetics: our window into the goals and strategies of the central nervous system. *Behav Brain Res* 67: 111–120, 1995.